SSS-R-77-3205

FE-1770-26
Distribution Category UC-90c

COMPUTER MODELING OF COAL GASIFICATION REACTORS

Quarterly Technical Progress Report
For Period January 1, 1977 - March 31, 1977

Thomas R. Blake

Systems, Science and Software
P. O. Box 1620
La Jolla, California 92038

May 1977

PREPARED FOR THE UNITED STATES
ENERGY RESEARCH AND DEVELOPMENT ADMINISTRATION

Under Contract No. E(49-18)-1770

TABLE OF CONTENTS

I. OBJECTIVE AND SCOPE OF WORK

The purpose of this program is to develop and apply, over three years, accurate and general computer models that will expedite the development and aid in the optimization and scale-up of reactors for coal gasification. Initial applications will be to fluidized bed gasification processes; subsequently both entrained flow reactors and fast fluidized beds will be examined.

During the first year, work will be initiated on the fluidized bed model in the areas of multiphase fluid flow without chemical reactions, and chemical reactions without fluid flow. The models, developed to represent these aspects of gasification processes, will be combined in the second year of the program into a numerical model of reactive flows in fluidized beds. This model will provide a time-dependent field description of fluidized bed flows in two space dimensions. Calculations will be performed with the prototype code during the first and second years to verify the accuracy of the formulations employed and, in the second year, these calculations should provide preliminary results relevant to coal gasifications. During the second year a computer model for entrained flow gasifiers will be formulated and the chemistry defined; this model will provide a field description of entrained flows in two space dimensions. Nonreactive flow calculations will be performed for entrained flow processes at the end of the second year.

In the third year the application of the fluidized bed computer model to specific gasifier processes will be extended and a computational model which includes three-dimensional effects will be developed. Also, during this third year the coal chemistry will be combined with the entrained flow computer model and some calculations of such gasifier configurations will be performed.

II. SUMMARY OF PROGRESS TO DATE

This was the third quarter in the second year of research to develop and apply computer codes, based upon continuum theories of multiphase flows, to the performance of fluidized bed and entrained flow coal gasification reactors. Research was active in several areas.

The research on the fluidized bed model was directed to the continued development of the chemistry for steam-oxygen gasification and to the incorporation of that chemistry into the numerical formulation. In addition, theoretical studies were continued or initiated on compressibility effects in fluidized beds, mechanical interaction functions, constitutive relationships and particle size effects.

The work on the entrained flow model included a continued formulation of the equations for turbulent gas-solid particle motion, the examination of chemical kinetics and the successful completion of a model computer code appropriate to representing transient entrained flows. This latter code, which involves a finite element-finite difference formulation has been applied to study swirling flows of a compressible viscous gas.

III. DETAILED DESCRIPTION OF TECHNICAL PROGRESS

3.1 TASK 00 - MANAGEMENT, DOCUMENTATION AND CONSULTING

A paper, "A Numerical Model of Gas Fluidized Beds," was accepted for publication in the AIChE Progress Symposium Series. In addition, a preliminary abstract, "A Numerical Simulation Model for Entrained Flow Coal Gasification, the Hydrodynamical Model", was submitted to the Symposium on Alternate Energy Sources, Miami Beach, Florida, December, 1977.

On January 6, 1977, Mayo Carrington visited La Jolla and reviewed the technical progress on the project. The incorporation of the steam-oxygen gasification chemistry into the fluidized bed code and the numerical formulations of both fluidized bed and entrained flow codes was discussed.

Professor C. Y. Wen of West Virginia University visited S^3 late in February for two days of discussion on coal chemistry and fluidized beds. A subcontract to West Virginia University was approved by ERDA and signed in March. This subcontract, with Professor Wen as the Principal Investigator, provides for the development of a homogeneous reactor model of steam-oxygen gasification. The model will be used in studies of chemical parameters related to the description of such processes.

Professor Paul A. Libby, of the University of California at San Diego, continued his research on two subjects related to entrained flows; the evolution of particle size distribution in dilute entrained flows and the coupling of transport phenomena and homogeneous/heterogeneous reactions associated with combustion of individual char particles. In this latter study, the influence of volatiles transport and combustion in the gas layer adjacent to the particle, upon both the heterogeneous reactions and the transport of reactants, is being investigated.

Consulting agreements between S^3 and Professor Joseph Yerushalmi of the City University of New York and Professor Julius Siekmann of the Technische Hochschule, Darmstadt, were approved by ERDA.

3.2 TASK 01 - FLUIDIZED BED COAL GASIFICATION MODEL

The research on the fluidized bed model was primarily directed to the continued development of the chemistry for steam-oxygen gasification and to the incorporation of this

chemistry into the numerical formulation. In addition, theoretical studies were initiated or continued on spatial averaging for compressible gas fluidized media, mechanical interaction functions, constitutive relationships and particle size effects.

The formulation of the chemistry for both gasification and combustion of char was continued. A previous model [Blake, 1977] for the heterogeneous reactions, species transport and homogeneous reactions for combustion of a char particle was extended to include the presence of ash. This was accomplished with a formulation based upon the concept of an unreacted-shrinking core model wherein the initial distribution of carbon and ash are assumed to be uniform throughout the particle. The oxidation of the carbon occurs at a reaction front which propagates into the particle, leaving an external layer of ash. When the carbon is consumed, there remains a particle of ash which is, naturally, less dense than the char particle, but which has the original external particle radius. In addition to the rate controlling processes of the kinetics at the reaction front and mass transport between the external particle surface and the ambient gas, the diffusion of reactants within the ash layer influences the reaction rate. Since we are using a single Arrhenius rate expression for the kinetics, where we assume adsorption dominance [Blake, 1977], this means that there are, three velocity coefficients associated with the overall rate expression for this shrinking core model. Within the context of the external ash layer and its tendency to inhibit transport we have further assumed that the heterogeneous reaction is essentially carbon and oxygen producing carbon dioxide. In Blake [1977], we discussed the homogeneous oxidation of carbon monoxide [c.f., Hottel, 1965]. However, this reaction should proceed to completion very close to the particle surface or within the porous matrix of the particle. Hence, for simplicity at this point, we consider that carbon oxidizes to carbon dioxide and this latter product enters the gas phase.

Again, the overall reaction rate (gms of carbon removed/cm^2 or particle surface area/sec) for a single particle, when summed over all local particles, provides a mass source for the differential equations describing conservation of mass. Any homogeneous reactions are represented by volumetric source terms in the conservation of mass for the respective gas species. The influence of both heterogeneous and homogeneous reactions upon the energy conservation is implicitly contained in a combined energy balance equation for the solid and gas phases and is explicitly accounted for in a Lagrangian energy balance for individual particles. In the case of local temperature equilibrium between the solid particles and

gas only the total energy equation is required to specify the energy conservation.

We have also formulated models for the heterogeneous gasification reactions: carbon-steam and carbon-carbon dioxide. For the temperature range appropriate to gasification these reactions can be approximately described with a single Arrhenius expression which is first order in the partial pressure of the reactant species in the gas phase. We are examining the application of a solid particle-gas exchange model to describe the interphase mass and energy exchange for these essentially volumetric reactions.

Within the context of the heterogeneous and homogeneous reactions for a single char particle we are examining, with a detailed theoretical analysis, these kinetics and also the transport of reactants and products in the neighborhood of a single particle. This analysis, which is initially for the stagnation region of a particle, provides a description of the coupled diffusion, convection and chemical reactions in the film around the particle. In particular, we are examining finite rate, equilibrium and frozen chemical descriptions for the homogeneous reactions and finite rate chemistry for the heterogeneous reactions associated with char oxidation. We wish to understand the relative influences of such heterogeneous reactions as carbon-oxygen and carbon-carbon dioxide in different ambient environments and to determine the effect of homogeneous reactions and species transport upon the control of the rate of reaction.

The incorporation of the chemistry and the species transport into the numerical description of fluidized bed flows was initiated and continues. This introduction of chemical reactions and multiple species requires several modifications to the existing computer code [Blake, et al., 1976]. We have already noted that the heterogeneous and homogeneous reactions provide source terms in the conservation of mass relationships. Further, instead of a single gas species we must now consider n (where n may be six) species to represent the dynamics of gas flow. The mass of the char particles changes with heterogeneous reaction; hence, the histories of the particle masses must be "remembered" by the numerical formulation. To model this flow, a finite difference implicit method, wherein conservation equations for species mass are solved simultaneously with the conservation of momentum and energy for the solid and gas phases, is being used. The initial application of this code will be to examine the combustion reactions and the associated mass transport. We expect that the fully implicit method for treatment of species transport is essential to describe such highly exothermic and rapid

processes. We note, however, that the complete description of those processes, which like gasification, occur on longer time scales and which require the description of a large number of gas species, may require lengthy computer calculations with such a treatment. Within this context we are exploring other theoretical and numerical formulations of these coupled flows.

Theoretical work on the equations of fluidized beds continued. A formulation of the conservation equations based upon density weighting of the velocity and energy variables has provided important insight into the incorporation of higher order compressible effects into the conservation equations. Further, a formalism which describes the influence of dispersion upon the gas and solid stress tensors has been developed. This latter relationship should be useful, for example, in providing a more complete description of the rheology of the solid phase in the continuum model of fluidized beds.

The theoretical formulation describing the relative transport of particles of different sizes in the fluidized bed was continued. We briefly discussed this formulation in the last Quarterly Technical Progress Report [Blake, 1977]; in essence, the properties of the fluidized bed which depend upon particle size and relate to the mechanical particle-particle and particle-gas interactions such as the solid phase viscosity, solid pressure and the solid particle-gas drag relationships are determined by the average of the particle size distribution. Then, the motion of each discrete particle size, with respect to the average bed, is calculated by dynamic relationships, which account for the interaction of this particle "bin" with the average bed.

3.3 TASK 02 - ENTRAINED FLOW COAL GASIFICATION MODEL

The research on the entrained flow model includes a continued formulation of the equations for turbulent gas-solid particle motion, the continuation of a theoretical description of particle size effects, initiation of an examination of chemical kinetics, and the successful completion of a model computer code appropriate to representing transient entrained flows. This latter code, which uses a finite element-finite difference formulation, was used to study swirling flows of a viscous compressible gas in two spatial dimensions. Subsequently (past seventh quarter), this code has been further developed to include particle motions.

In the fifth and sixth quarters of this contract we respectively developed balance equations for gas-particle

flows without turbulence and with turbulence. The closure of these turbulence equations has been partially considered [Blake, 1977] and in the present quarter we completed the derivation of the relationships which are necessary to insure closure of the field equations for entrained flow. This formulation of closure is based upon a second order (eddy viscosity) scheme which is a variation of that developed by Spalding and his coworkers for turbulence in fluids without particles (c.f., Launder and Spalding [1972]). Specifically, we base the closure upon the turbulent kinetic energies of the gas and solid phases and a single turbulent length scale, which, in turn, depends upon a turbulent dissipation rate. Differential equations describe the evolution of the turbulent kinetic energies and the dissipation rate. These differential equations are to be solved simultaneously with the conservation equations of mass, momentum and energy for the solid and gas phases. With the associated constitutive relationships, these differential equations comprise the closure of the field equations for entrained flow processes. A discussion of these equations is presented in Appendix A. The complete mathematical specification of the appropriate initial-boundary value problem requires the establishment of a boundary and initial conditions. Some of these conditions are readily derived but care is required in the specification of such conditions on the turbulent kinetic energy, the dissipation rate, etc. This formulation is being developed at the present time.

The study of the evolution of particle size distribution, in very dilute entrained flows, was continued. Most of the effort was devoted to modeling correlations which occur in the equation for particle size distribution with turbulence (c.f., Appendix D in Blake [1977]) and in developing more detailed representations of mass loss from a single particle of carbon which is experiencing oxidation reactions.

We initiated studies of chemical kinetics and transport related to devolatilization, oxidation and gasification of pulverized coal/char in an entrained flow environment. We expect that our present studies of such processes in fluidized beds will be very useful with respect to both oxidation and gasification modeling. However, many aspects of devolatilization and subsequent combustion of the volatiles must be considered with regard to the particular nature of entrained flow systems.

A rather advanced numerical code has been developed to treat transient multi-dimensional flow of a viscous compressible gas. This code uses both finite element and finite difference techniques. In particular, the geometric

advantages related to zone size distribution and zone shape, which are peculiar to finite element techniques, are retained to provide a good description of the geometries, such as walls, channels and nozzles, which are important to internal flows in gasifiers. The finite difference techniques are used in the major numerical solutions of the differential equations; there is some finite element methodology applied in the definition of local variables in terms of the element and nodal values. Aspects of this numerical model together with some representative calculations are shown in Appendix B.

We have decided to use the basic numerical approach as represented by this finite element-finite difference code in the development of a code to model turbulent entrained flows. To this end we have since added the conservation equations for the solid phase and have performed some preliminary test calculations with this modified code. The turbulence model will be included in this numerical formulation subsequent to the use of the code in representing some exact solutions of gas-solid particle flows.

IV. CONCLUSIONS

In summary, we note the following aspects of our modeling effort.

- The chemistry and species transport associated with steam oxygen gasification processes is being incorporated into the numerical model for fluidized beds. This formulation includes a fully implicit solution of the coupled species transport and conservation of momentum and energy for the two phase continuum model. We are also investigating other theoretical and numerical formulations of these coupled flows.

- A preliminary version of a numerical model for entrained flows has been developed. This model incorporates both finite element and finite difference methodology to represent transient multidimensional flows.

APPENDIX A

DERIVATION OF EQUATIONS FOR TURBULENT ENTRAINED FLOWS

In Blake [1977], a derivation of the turbulent form of the conservation equations for the solid particle-gas flows appropriate to entrained processes was presented. In many of the equations derived there, terms involving turbulent fluctuations arose. While several of these terms were discussed and then either modeled or discarded, others remained. In order to effect closure of this set of turbulent equations, one must deal with these remaining terms.

We have elected to use a second-order (eddy viscosity) turbulence closure scheme which is a variation of the k-ε model developed by the Spalding group at Imperial College, London (see, for example, Launder and Spalding [1972]). We now turn to applying it to the turbulence terms remaining in the mean conservation equations.

In the conservation of mean gas momentum equation (Eq. C.3b of Blake [1977]) one turbulence term, representing the net diffusion of mean momentum by the turbulence field (i.e., the divergence of the Reynolds' stress), remained. We model the gaseous Reynolds' stress by:

$$\overline{\rho_f v_i'' v_j''} = - \mu_{tf} \left(\frac{\partial \tilde{v}_i}{\partial x_j} + \frac{\partial \tilde{v}_j}{\partial x_i} \right) + \frac{2}{3} \left(\mu_{tf} \frac{\partial \tilde{v}_k}{\partial x_k} + \bar{\rho}_f \tilde{k}_f \right) \delta_{ij} \quad \text{(A.1)}$$

where μ_{tf} = turbulent (eddy) dynamic viscosity coefficient and $\tilde{k}_f = (\overline{\rho_f v_i''^2})/(2\bar{\rho}_f)$ = Favre-averaged fluid turbulent kinetic energy. One should note that the first term on the RHS of Eq. (A.1) is the classical Navier-Stokes shear stress but with μ_{tf} replacing the laminar dynamic viscosity coefficient. The latter two terms appear so that the first invariant of the Reynolds' stress tensor and the modeled form for it are identical and represent the turbulent

analogues of bulk viscous stress (with $\lambda_{tf} = 2/3\ \mu_{tf}$) and pressure, respectively.

Dealing with the solid Reynolds' stress term in Eq. (C.4b) of Blake [1977] in the same manner, we have:

$$\overline{\rho_p u_i'' u_j''} = - \mu_{tp} \left(\frac{\partial \tilde{u}_i}{\partial x_j} + \frac{\partial \tilde{u}_j}{\partial x_i} \right) + \frac{2}{3} \left(\mu_{tp} \frac{\partial \tilde{u}_k}{\partial x_k} + \bar{\rho}_p \tilde{k}_p \right) \delta_{ij} \qquad (A.2)$$

where μ_{tp} and $\tilde{k}_p$ are the solid analogues of μ_{tf} and $\tilde{k}_f$.

The conservation of gaseous species mass equation (Eq. C.5b of Blake [1977]) contains a term which represents the net diffusion of the mass of species α by the turbulence field. We model the flux in a Fickian manner so that:

$$\overline{\rho_f F_\alpha'' v_i''} = - \frac{\mu_{tf}}{\sigma_F} \frac{\partial \tilde{F}_\alpha}{\partial x_i} \qquad (A.3)$$

where σ_F = turbulent Schmidt number (for species diffusion) which will be assumed constant and applicable for all α.

The combined energy equation (Eq. C.14b of Blake [1977]) contains two turbulent terms representing the net diffusion of gaseous and solid internal energy, respectively, by their respective turbulence fields. We model these terms analogously to species mass so:

$$\overline{\rho_f e_f'' v_i''} = - \frac{\mu_{tf}}{\sigma_e} \frac{\partial \tilde{e}_f}{\partial x_i} \qquad (A.4a)$$

$$\overline{\rho_p e_p'' u_i''} = - \frac{\mu_{tp}}{\sigma_e} \frac{\partial \tilde{e}_p}{\partial x_i} \qquad (A.4b)$$

where σ_e = turbulent Prandtl number (for energy) which is assumed constant and applicable for all gaseous and solid materials.

Equations (A.1) - (A.4) permit elimination of the remaining turbulent correlation terms but closure is not yet complete since μ_{tf}, μ_{tp}, $\tilde{k}_f$ and $\tilde{k}_p$ remain to be specified. It is known that the eddy viscosity can be characterized by the use of suitable scales of turbulent intensity and turbulent length. Prandtl [1945] and Kolmogorov [1942] suggest the turbulent kinetic energy as a suitable scale for turbulent intensity, but the specification of the turbulent length scale has been somewhat more elusive since, unlike kinetic energy, it is not a conserved quantity. Consequently, a search was conducted for a conserved property which was proportional to <u>both</u> turbulent intensity and length so that it and turbulent kinetic energy would constitute linearly independent quantities from which the turbulent length scale could be deduced. Harlow and Nakayama [1968] and others suggested the turbulent dissipation rate, ε, and Jones and Launder [1972] determined that it gave better results than others investigated. Thus, we take

$$\mu_{tf} \equiv C_\mu \, \bar{\rho}_f \tilde{k}_f^2 / \tilde{\varepsilon} \tag{A.5}$$

where

$$\tilde{\varepsilon} \, \frac{\overline{\rho_f \varepsilon}}{\bar{\rho}_f} = \frac{1}{\bar{\rho}_f} \left[\overline{\phi \mu_\ell \left(\frac{\partial v_i''}{\partial x_j} \right) \left(\frac{\partial v_i''}{\partial x_j} + \frac{\partial v_j''}{\partial x_i} \right)} \right] = \text{Favre-averaged fluid turbulent dissipation rate} \tag{A.6}$$

and, μ_ℓ = fluid laminar dynamic viscosity coefficient. In writing Eq. (A.5), we have implicitly set the gaseous turbulent length scale, ℓ_f, as:

$$\ell_f \sim \tilde{k}_f^{3/2} / \tilde{\varepsilon} \tag{A.7}$$

We will now assume that the solid turbulent length scale, ℓ_p, is identical to the gaseous one. The rationale is that

if the particles are much smaller than ℓ_f, they "see" only a sea that is the gaseous turbule of scale, ℓ_f, and move about with it except that they lag somewhat in acceleration. Thus, the solid turbulent length scales are identical. This is, of course, an approximation that only subsequent experience will confirm or deny. If we now take $\ell_p = \ell_f$, we have:

$$\mu_{tp} = \mu_{tf} \, (\bar{\rho}_p/\bar{\rho}_f) \, (\tilde{k}_p/\tilde{k}_f)^{1/2} \tag{A.8}$$

This leaves only $\tilde{k}_f$, $\tilde{k}_p$, and $\tilde{\varepsilon}$ unspecified. We now turn to developing model conservation equations for these three quantities. Since the starting points for these model equations are Eqs. (C-1)-(C-4) of Blake [1977], we reproduce those here (except that in Eq. (C.3) we have added back the laminar viscous shear term previously discarded):

$$\frac{\partial \rho_f}{\partial t} + \frac{\partial (\rho_f v_j)}{\partial x_j} = S \tag{C.1}$$

$$\frac{\partial \rho_p}{\partial t} + \frac{\partial (\rho_p u_j)}{\partial x_j} = - S \tag{C.2}$$

$$\frac{\partial (\rho_f v_i)}{\partial t} + \frac{\partial (\rho_f v_i v_j)}{\partial x_j} = - \frac{\partial P}{\partial x_i} - G(\mu_\ell, r) \rho_p (v_i - u_i) + \rho_f g_i + \frac{\partial}{\partial x_j} \left[\mu_\ell \left(\frac{\partial v_i}{\partial x_j} + \frac{\partial v_j}{\partial x_i} \right) \right] \tag{C.3}$$

$$\frac{\partial (\rho_p u_i)}{\partial t} + \frac{\partial (\rho_p u_i u_j)}{\partial x_j} = G(\mu_\ell, r) \rho_p (v_i - u_i) + \rho_p g_i \tag{C.4}$$

Let us multiply Eq. (C.1) by v_i and subtract the result from Eq. (C.3) to yield:

$$\rho_f \frac{\partial v_i}{\partial t} + \rho_f v_j \frac{\partial v_i}{\partial x_j} = - \frac{\partial P}{\partial x_i} - G(\mu_\ell, r)\rho_p(v_i - u_i)$$

$$+ \rho_f g_i - S v_i + \frac{\partial}{\partial x_j}\left[\mu_\ell\left(\frac{\partial v_i}{\partial x_j} + \frac{\partial v_j}{\partial x_i}\right)\right] \quad (A.9)$$

Now, multiply Eq. (A.9) by v_i'' and recalling that $v_i = \tilde{v}_i + v_i''$, we get

$$\rho_f \frac{\partial(\frac{v_i''^2}{2})}{\partial t} + \rho_f v_j \frac{\partial(\frac{v_i''^2}{2})}{\partial x_j} + \rho_f v_i'' \frac{\partial \tilde{v}_i}{\partial t} + \rho_f v_i'' v_j \frac{\partial \tilde{v}_i}{\partial x_j}$$

$$= - v_i'' \frac{\partial P}{\partial x_i} - G(\mu_\ell, r)\left[\rho_p v_i''(\tilde{v}_i - \tilde{u}_i) + \rho_p v_i''^2\right.$$

$$\left. - \rho_p u_i'' v_i''\right] + \rho_f v_i'' g_i - S v_i v_i''$$

$$+ v_i'' \frac{\partial}{\partial x_j}\left[\mu_\ell\left(\frac{\partial v_i}{\partial x_j} + \frac{\partial v_j}{\partial x_i}\right)\right] \quad (A.10)$$

Multiply Eq. (C.1) by $v_i''^2/2$, add to (A.10), and time average the result to get:

$$\frac{\partial(\bar{\rho}_f \tilde{k}_f)}{\partial t} + \frac{\partial(\overline{\rho_f v_j k_f})}{\partial x_j} + \overline{\rho_f v_i'' v_j''} \frac{\partial \tilde{v}_i}{\partial x_j} = - \overline{v_i'' \frac{\partial P}{\partial x_i}}$$

$$- \overline{\mu_\ell \left(\frac{\partial v_i''}{\partial x_j}\right)\left(\frac{\partial v_i''}{\partial x_j} + \frac{\partial v_j''}{\partial x_i}\right)} - G(\mu_\ell, r)\left[\overline{\rho_p v_i''(\tilde{v}_i - \tilde{u}_i)}\right.$$

$$\left. + 2\,\overline{\rho_p k_f} - \overline{\rho_p u_i'' v_i''}\right] - \overline{S k_f} + \overline{v_i''} \frac{\partial}{\partial x_j}\left[\mu_\ell\left(\frac{\partial \tilde{v}_i}{\partial x_j} + \frac{\partial \tilde{v}_j}{\partial x_i}\right)\right]$$

$$+ \frac{\partial}{\partial x_j}\left[\mu_\ell \frac{\partial \bar{k}_f}{\partial x_j}\right] + \frac{\partial}{\partial x_j}\left[\mu_\ell \overline{v_i'' \frac{\partial v_j''}{\partial x_i}}\right] \quad (A.11)$$

Note that the gravity term has disappeared so that in the Favre-averaged formulation, bouyancy does not directly affect the turbulent kinetic energy. Let us expand the second term in Eq. (A.11), recalling the definition of $\tilde{k}_f$ and rearrange to get:

$$\frac{\partial(\bar{\rho}_f \tilde{k}_f)}{\partial t} + \frac{\partial(\bar{\rho}_f \tilde{v}_j \tilde{k}_f)}{\partial x_j} = - \frac{\partial(\overline{\rho_f v_j'' k_f''})}{\partial x_j} - \overline{\rho_f v_i'' v_j''} \frac{\partial \tilde{v}_i}{\partial x_j}$$

$$- \overline{\mu_\ell \left(\frac{\partial v_i''}{\partial x_j}\right)\left(\frac{\partial v_i''}{\partial x_j} + \frac{\partial v_j''}{\partial x_i}\right)}$$

$$- G(\mu_\ell, r) \left[\overline{\rho_p v_i''} (\tilde{v}_i - \tilde{u}_i) + 2 \overline{\rho_p k_f}\right.$$

$$\left. - \overline{\rho_p u_i'' v_i''}\right] - \overline{v_i'' \frac{\partial P}{\partial x_i}} - \overline{S k_f}$$

$$+ \overline{v_i''} \frac{\partial}{\partial x_j} \left[\mu_\ell \left(\frac{\partial \tilde{v}_i}{\partial x_j} + \frac{\partial \tilde{v}_j}{\partial x_i}\right)\right] + \frac{\partial}{\partial x_j} \left[\mu_\ell \frac{\partial \bar{k}_f}{\partial x_j}\right]$$

$$+ \frac{\partial}{\partial x_j} \left[\mu_\ell \overline{v_i'' \frac{\partial v_j''}{\partial x_i}}\right] \qquad \text{(A.11a)}$$

Equation (A.11a) represents the full, unmodeled gaseous (mean) turbulent kinetic energy conservation equation. Operating on Eqs. (C.2) and (C.4) in an analogous fashion yields the analogous solid equation:

$$\frac{\partial(\bar{\rho}_p \tilde{k}_p)}{\partial t} + \frac{\partial(\bar{\rho}_p \tilde{u}_j \tilde{k}_p)}{\partial x_j} = - \frac{\partial(\overline{\rho_p u_j'' k_p''})}{\partial x_j} - \overline{\rho_p u_i'' u_j''} \frac{\partial \tilde{u}_i}{\partial x_j} \qquad \text{(A.12)}$$

$$+ G(\mu_\ell, r) \left[\overline{\rho_p u_i'' v_i''} - 2 \bar{\rho}_p \tilde{k}_p\right] + \overline{S k_p}$$

The turbulent correlation terms in Eqs. (A.11a) and (A.12) must now be discarded or modeled.

Consistent with our previous assumptions [Blake, 1977], we believe the solid-gas mass exchange will be relatively small so the associated turbulent kinetic energy exchange should be negligible. Thus, we discard $\overline{Sk_f}$ and $\overline{Sk_p}$. We previously discarded the $\overline{P\ \partial v_i''/\partial x_i}$ term from the mean energy equation (Blake [1977]) and, for the same reasons, will discard the $\overline{v_i''\ \partial P/\partial x_i}$ term from Eq. (A.11a). The last three terms in Eq. (A.11a) represent mechanical work and diffusion terms by laminar viscous action. Similar terms will appear involving the turbulent viscous action which is usually about 100 times larger, thus we shall discard all three terms. A comparison between the third term on the RHS of Eq. (A.11a) and Eq. (A.6) shows that it is really $\overline{\rho\varepsilon}$ which we shall approximate as $\overline{\rho_f\varepsilon}/\overline{\phi} = \overline{\rho}_f\tilde{\varepsilon}/\overline{\phi} = \overline{\rho}\tilde{\varepsilon}$. Note that the production terms contain the appropriate Reynolds' stress which has already been modeled in Eqs. (A.1) and (A.2). Similarly, if we simply consider k_f'', k_p'' as turbulent fluctuations in scalar quantities, the diffusion terms are completely analogous to species mass fraction and specific internal energy and can be modeled in analogous fashion. Thus, we have:

$$\overline{\rho_f v_i'' k_f''} = - \frac{\mu_{tf}}{\sigma_k} \frac{\partial \tilde{k}_f}{\partial x_i} \tag{A.13a}$$

$$\overline{\rho_p u_i'' k_p''} = - \frac{\mu_{tp}}{\sigma_k} \frac{\partial \tilde{k}_p}{\partial x_i} \tag{A.13b}$$

where σ_k = turbulent Prandtl/Schmidt number for turbulent kinetic energy and is assumed constant and applicable to both solid and gas. The only terms remaining to be modeled arise from the Stokes' drag law. Examination of the origin of these terms reveals that they are all part of a

$-G(\mu_\ell, r)\ \overline{\rho_p (v_i - u_i)^2}$ term in a total kinetic energy equation. Thus, they represent portions of the dissipation into heat due to interactions between the gas and solid, mean and turbulent fields. According to the entity (e.g., solid mean kinetic energy, gas turbulent kinetic energy, etc.) equation being considered, the terms appearing represent the kinetic energy being gained or lost by transfer between that entity and the other three as well as that lost due to dissipation into heat. The first term in the [] of Eq. (A.11a) represents an interaction between the mean and turbulent velocity fields; an analogous term would appear in the [] of Eq. (A.12) except that it vanishes identically in the Favre-averaged form because $\overline{\rho_p u_i''} \equiv 0$. For this reason we suspect the term in Eq. (A.11a) may be very nearly zero and so have decided to discard it. The remaining terms represent interactions between the solid/gas turbulence fields with some transfer and some dissipation. The fluctuation phase relationship between the two fields is important here. We have chosen, at least temporarily, to assume no phase shift which yields nearly the correct dissipation but may apportion the turbulent kinetic energy incorrectly between the solid and gas. Further analysis is continuing in an attempt to quantify the phase shift, but, in the interim, we have chosen to model the term as:

$$\overline{\rho_p k_f} = \bar{\rho}_p \tilde{k}_f \quad \text{(which assumes } \overline{\rho_p k_f''} \equiv 0\text{)} \tag{A.14a}$$

$$\overline{\rho_p u_i'' v_i''} = 2\, \bar{\rho}_p\, (\tilde{k}_f \tilde{k}_p)^{1/2} \tag{A.14b}$$

Substituting all of the modeled terms into Eq. (A.11a) yields:

$$\frac{\partial(\bar{\rho}_f\tilde{k}_f)}{\partial t} + \frac{\partial(\rho_f\tilde{v}_i\tilde{k}_f)}{\partial x_i} = \frac{\partial}{\partial x_i}\left(\frac{\mu_{tf}}{\sigma_k}\frac{\partial\tilde{k}_f}{\partial x_i}\right) - \frac{2}{3}\frac{\partial\tilde{v}_j}{\partial x_j}\left(\mu_{tf}\frac{\partial\tilde{v}_j}{\partial x_j} + \bar{\rho}_f\tilde{k}_f\right)$$

$$+ \mu_{tf}\frac{\partial\tilde{v}_i}{\partial x_j}\left(\frac{\partial\tilde{v}_i}{\partial x_j} + \frac{\partial\tilde{v}_j}{\partial x_i}\right) - \bar{\rho}\,\tilde{\varepsilon}$$

$$- 2G(\mu_\ell, r)\left[\bar{\rho}_p\tilde{k}_f - \bar{\rho}_p(\tilde{k}_f\tilde{k}_p)^{1/2}\right] \qquad (A.15)$$

while substitution into Eq. (A.12) yields:

$$\frac{\partial(\bar{\rho}_p\tilde{k}_p)}{\partial t} + \frac{\partial(\bar{\rho}_p\tilde{u}_i\tilde{k}_p)}{\partial x_i} = \frac{\partial}{\partial x_i}\left(\frac{\mu_{tp}}{\sigma_k}\frac{\partial\tilde{k}_p}{\partial x_i}\right) + \mu_{tp}\frac{\partial\tilde{u}_i}{\partial x_j}\left(\frac{\partial\tilde{u}_i}{\partial x_j} + \frac{\partial\tilde{u}_j}{\partial x_i}\right)$$

$$- \frac{2}{3}\frac{\partial\tilde{u}_j}{\partial x_j}\left(\mu_{tp}\frac{\partial\tilde{u}_j}{\partial x_j} + \bar{\rho}_p\tilde{k}_p\right)$$

$$+ 2G(\mu_\ell, r)\ \left[\bar{\rho}_p(\tilde{k}_f\tilde{k}_p)^{1/2} - \bar{\rho}_p\tilde{k}_p\right] \qquad (A.16)$$

We now only need a model equation for $\tilde{\varepsilon}$ to close the set. Unfortunately, we have been unable, so far, to derive an exact equation for $\tilde{\varepsilon}$ that seems conveniently modelable. Consequently, we have chosen to follow the analogy with the other equations between the Favre-averaged form of the compressible equations and the incompressible form of the standard-averaged equations. This approach has been used recently by Kent and Bilger [1976] with quite reasonable success. Thus, we model the conservation equations for $\tilde{\varepsilon}$ as:

$$\frac{\partial(\bar{\rho}_f\tilde{\varepsilon})}{\partial t} + \frac{\partial(\bar{\rho}_f\tilde{v}_j\tilde{\varepsilon})}{\partial x_j} = \frac{\partial}{\partial x_j}\left(\frac{\mu_{tf}}{\sigma_\varepsilon}\frac{\partial}{\partial x_j}\right) + \frac{C_1\mu_{tf}\tilde{\varepsilon}}{\tilde{k}_f}\left(\frac{\partial\tilde{v}_i}{\partial x_j}\right)\left(\frac{\partial\tilde{v}_i}{\partial x_j} + \frac{\partial\tilde{v}_j}{\partial x_i}\right)$$

$$- \frac{\bar{\rho}_f\tilde{\varepsilon}}{3}\left(\frac{\partial\tilde{v}_j}{\partial x_j}\right) - \frac{2C_1\mu_{tf}\tilde{\varepsilon}}{3\tilde{k}_f}\left(\frac{\partial v_j}{\partial x_j}\right)^2 - \frac{C_2\bar{\rho}_f\tilde{\varepsilon}^2}{\tilde{k}_f} \qquad (A.17)$$

where σ_ε = turbulent Prandtl/Schmidt number for dissipation rate and is assumed constant and C_1, C_2 are empirical constants (may vary at low turbulence Reynolds' number).

The models presented in this appendix complete the turbulent closure of the field equations for entrained flow processes. With appropriate boundary and initial conditions, the system is properly specified and can be solved numerically. The specification of boundary and initial condition is, unfortunately, non-trivial and, therefore, will be left for the next report.

APPENDIX B

A FINITE DIFFERENCE/FINITE ELEMENT SOLUTION OF COMPRESSIBLE VISCOUS FLOW

The finite difference/finite element technique for solving the Navier-Stokes equations, described in the previous quarterly report [Blake, 1977], has been modified and implemented in a working computer code. The modifications consist of a change in the way in which velocity is updated and yield a finite difference treatment of the momentum equations. (We note that the numerical formulation in that previous report already contains a finite difference representation of the conservation of mass.) The finite element flexibility in zoning is retained.

The compressible Navier-Stokes code has been used to compute transient swirling flow in a circular vessel, shown in Figure B.1. The outer radius of the vessel is 30.48 cm, and an outlet at the center is modeled by a pressure boundary condition of 1.012×10^6 dynes/cm^2 (760 mm/Hg) applied on a circle of radius 7.62 cm. The air in the vessel is initially at density $\rho_0 = 1.213 \times 10^{-3}$ gm/cm^3 and temperature 18°C, with pressure $\rho_0 = 1.012 \times 10^6$ dynes/cm^2; the air is assumed to be an ideal gas with an adiabatic equation of state

$$p = p_0 \, (\rho/\rho_0)^{\gamma}$$

where $\gamma = 1.40$. The inlets are 7.62 cm wide, the inlet velocity is of magnitude 2038 cm/sec (Mach number 0.596),

and the velocities are directed so as to be tangent to the inner circular boundary.

The computational grid used in the calculation is shown in Figure B.2; it contains 720 elements, at which the fluid density and pressure are centered, and 780 nodes, at which velocity is centered. Figure B.3 shows the velocity vectors at time = 0; the inlet velocities are maintained at their time = 0 values throughout the calculation.

The development of the flow to near-steady state is shown in Figures B.4-B.8. In the early time flow pattern, Figure B.4, the fluid velocities at the outlet region are very uniform, and directed radially. Also, a small vortex region has developed to the left of each inlet. At t = 21.2 msec, Figure B.5, the effect of fluid advection has perturbed the velocity distribution in the outlet region, and the vortex regions have migrated somewhat toward the outlet.

By time = 41.2 msec, Figure B.6, the flow in the outlet region has reversed direction and is beginning to form a swirling pattern. The early-time vortex regions have migrated out of the grid. At time = 79.6 msec, Figure B.7, the steady state is nearly attained; the velocity pattern is very close to that at time = 147.4 msec, Figure B.8. At these late times, large recirculating flow regions have developed between the inlets. At time = 147.4 msec the time rate of angular momentum leaving the system is 14 percent greater than the time rate of angular momentum injected, but this "overshoot" is declining. This inequality is associated with shear stresses, numerical in origin, at the no-slip boundary of the vessel.

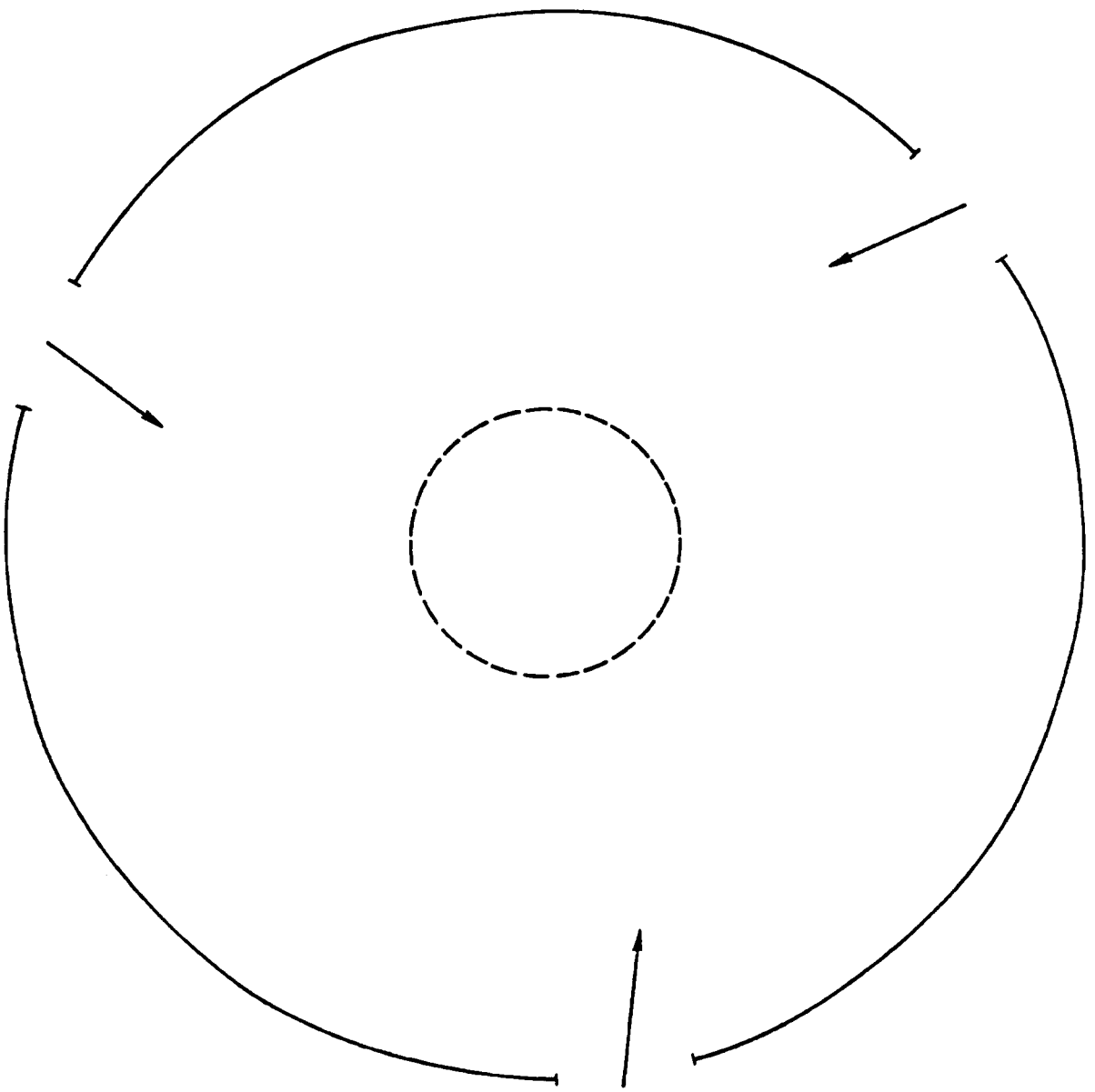

Figure B.1. Two-dimensional circular vessel.

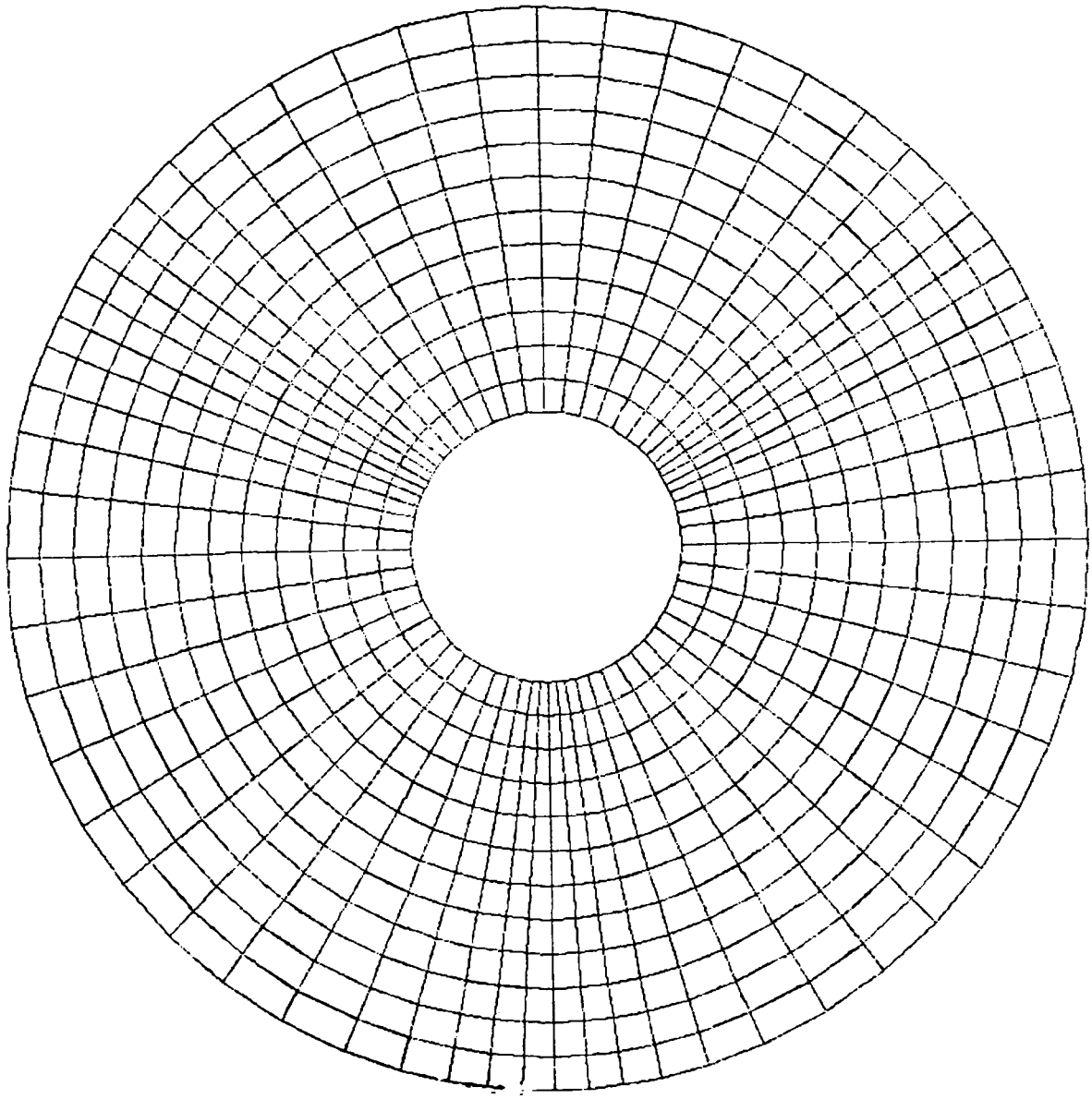

Figure B.2. Computational grid for swirling flow problem.

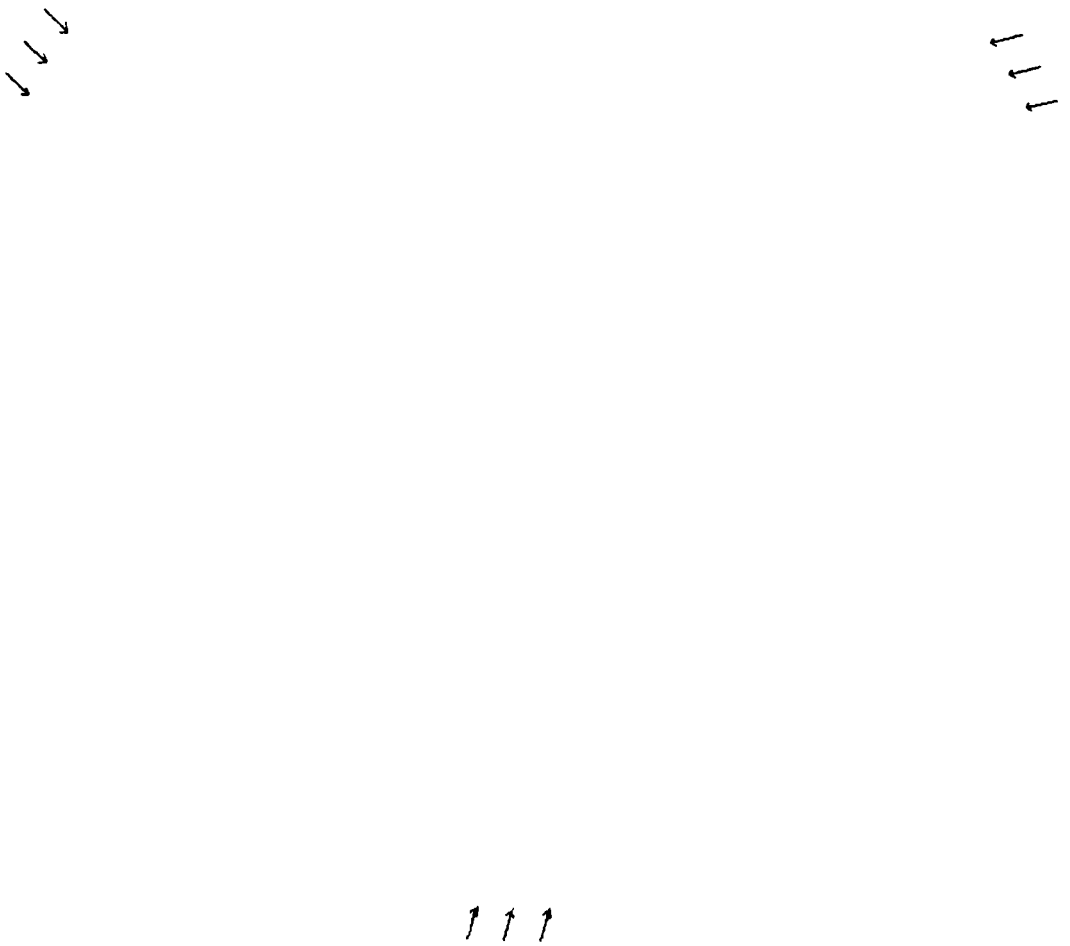

Figure B.3. Velocity vectors, swirling flow problem, time = 0.

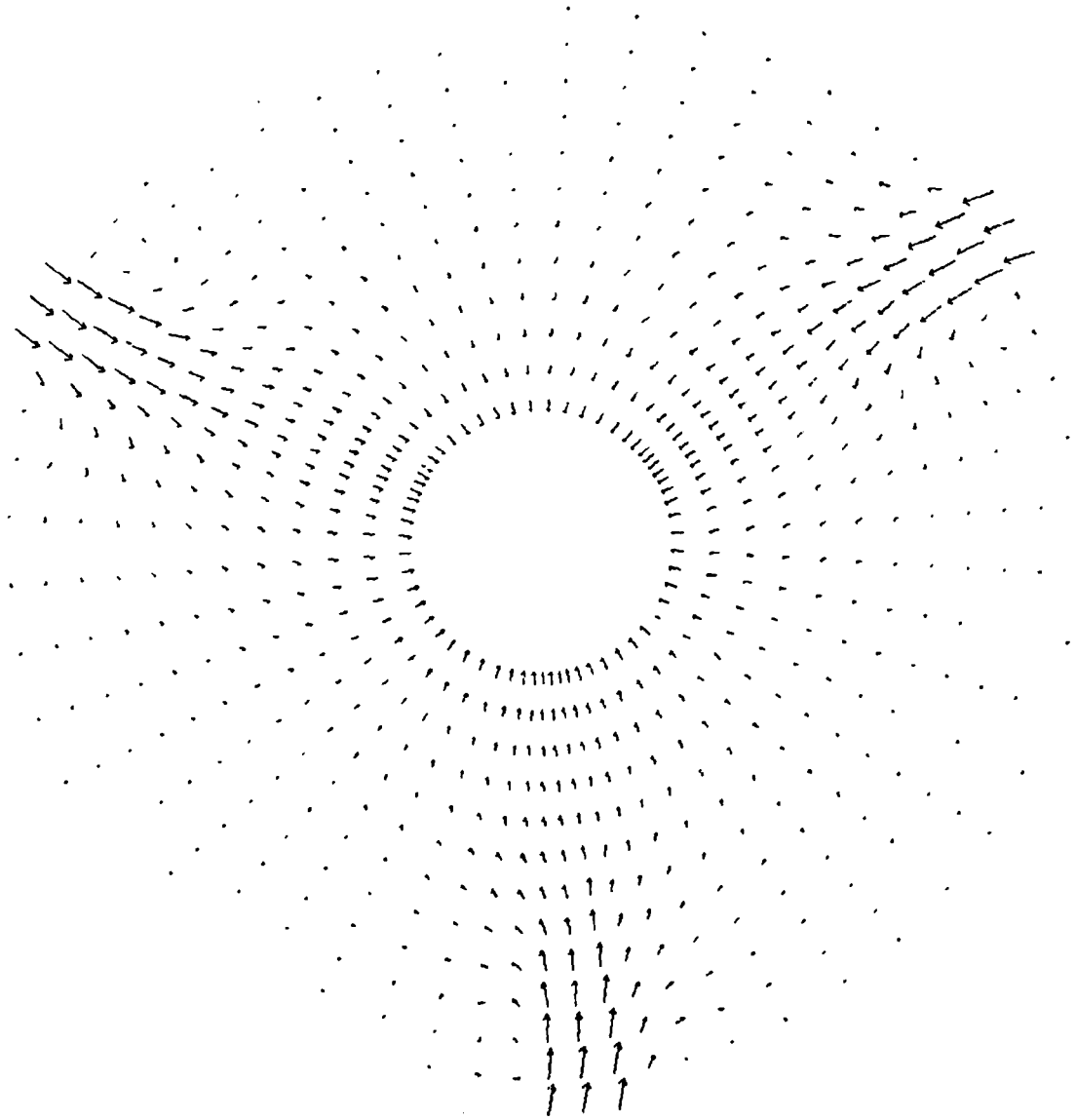

Figure B.4. Velocity vectors, swirling flow problem, time = 6.2 msec.

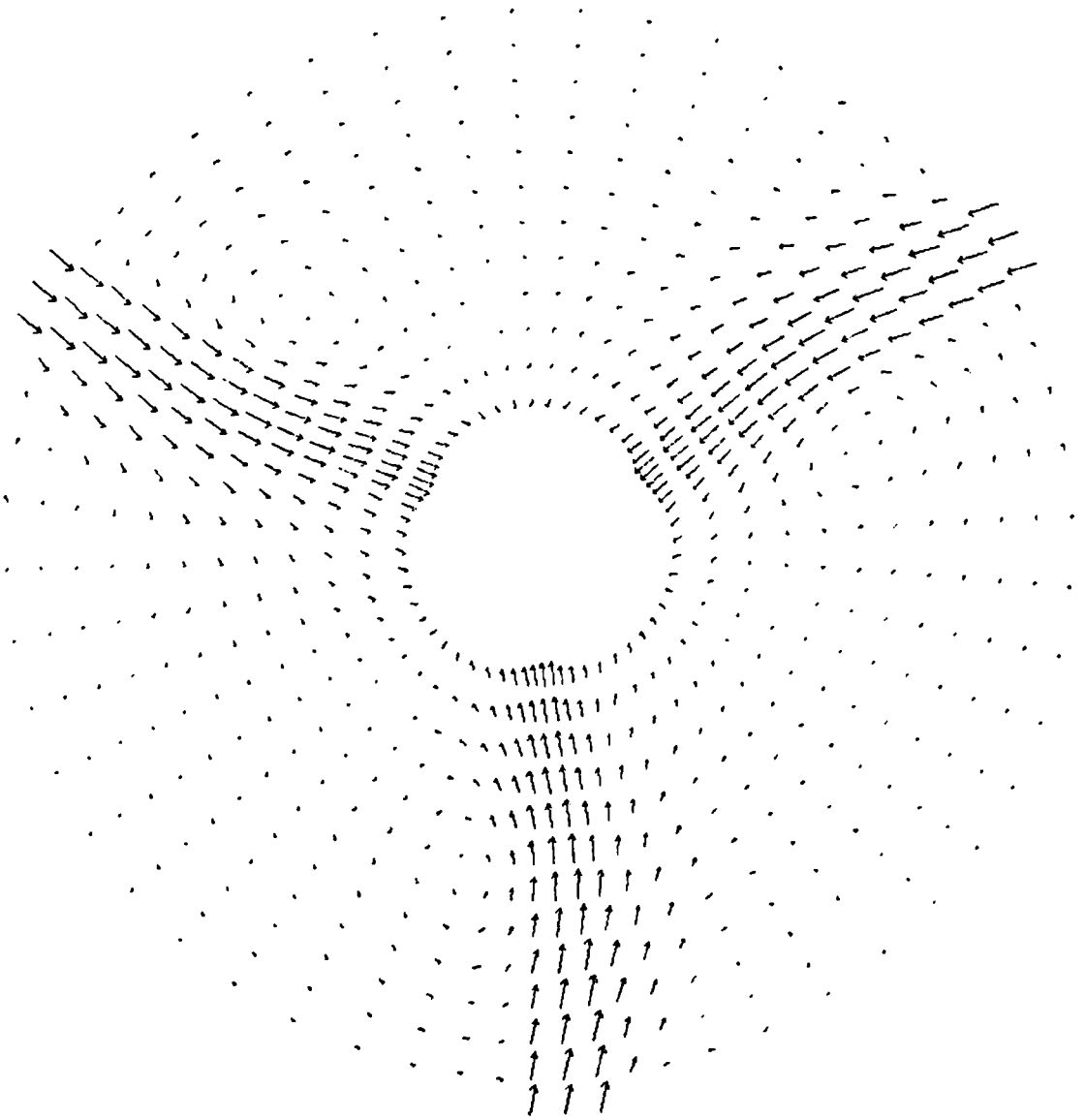

Figure B.5. Velocity vectors, swirling flow problem, time = 21.2 msec.

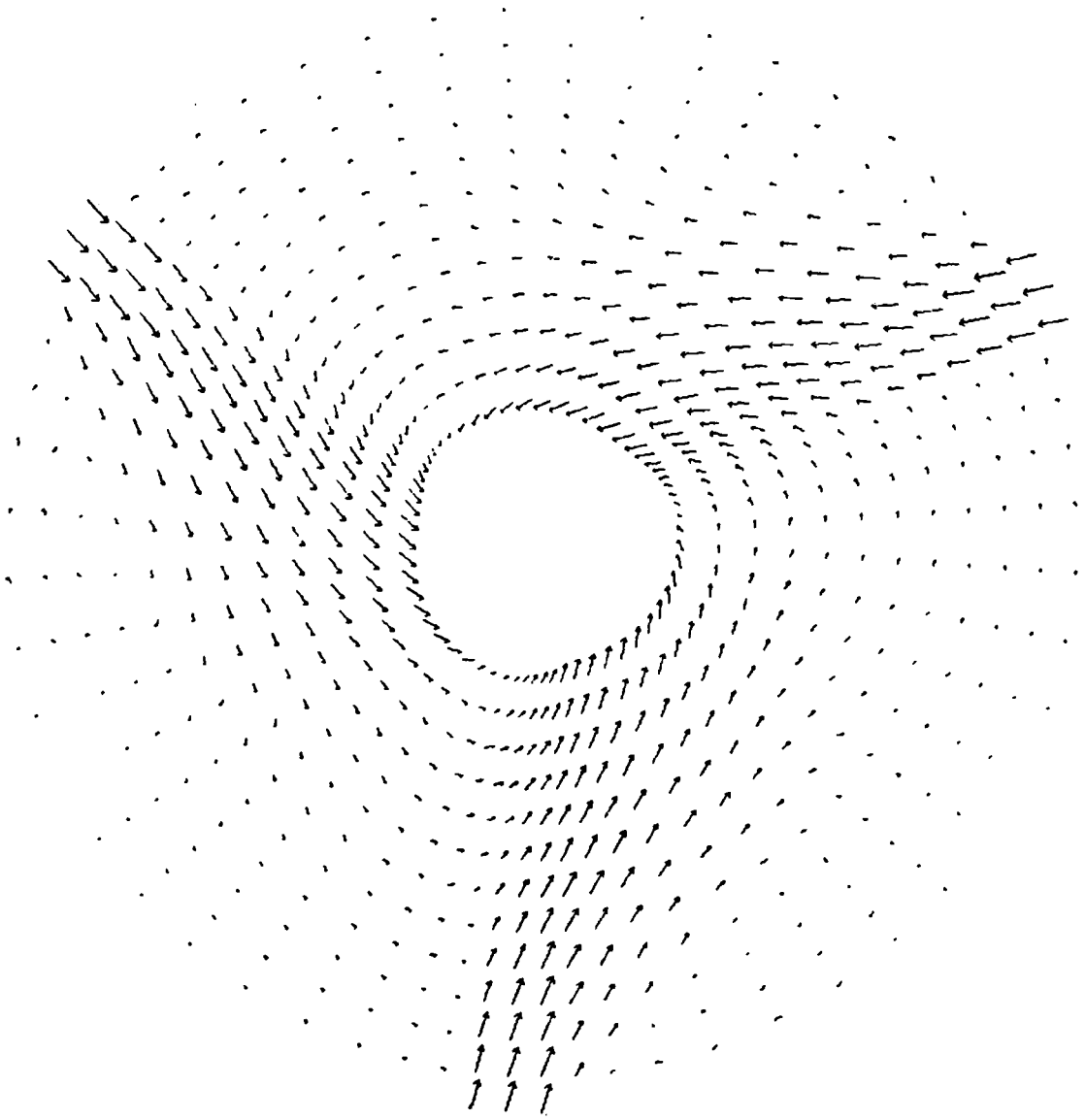

Figure B.6. Velocity vectors, swirling flow problem, time = 41.2 msec.

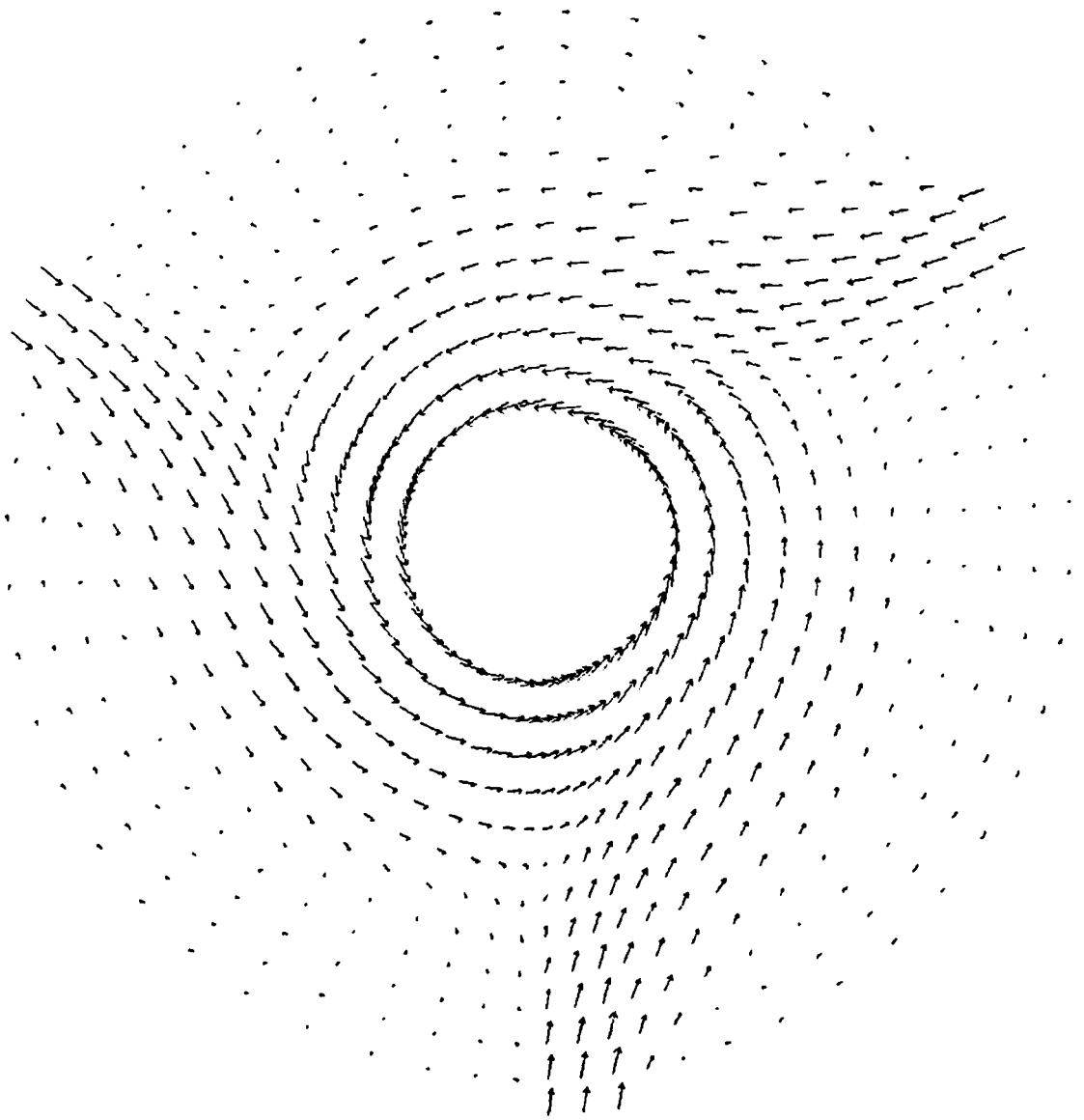

Figure B.7. Velocity vectors, swirling flow problem, time = 79.6 msec.

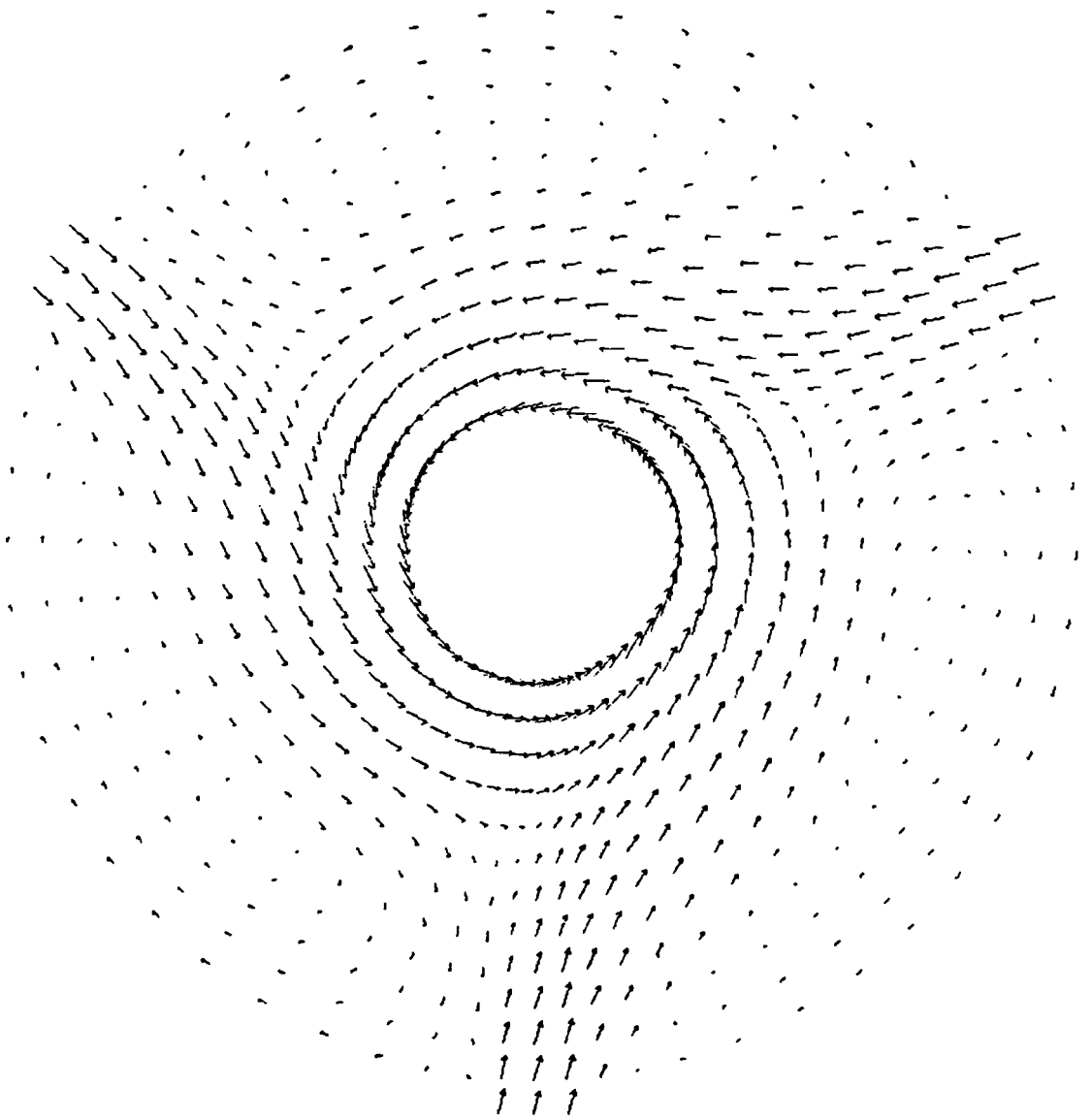

Figure B.8. Velocity vectors, swirling flow problem, time = 147.4 msec.

REFERENCES

Blake, T. R. [1976], Energy Research and Development Administrative Report FE 1770-19.

Blake, T. R. [1977], Energy Research and Development Administration Report FE 1770-23.

Blake, T. R., S. K. Garg, H. B. Levine and J. W. Pritchett [1976], Energy Research and Development Administration Report FE 1770-15.

Harlow, F. H. and P. I. Nakayama [1968], Los Alamos Scientific Laboratory Report LA-3854.

Hottel, H. C., G. C. Williams, N. M. Nerheim and G. R. Schneider [1965], Tenth International Symposium on Combustion, pp. 111-121.

Jones, W. P. and B. E. Launder [1972], Int. J. Heat Mass Transfer, 15, p. 301.

Kent, J. H. and R. W. Bilger [1976], University of Sydney, Charles Kolling Research Laboratory Technical Note F-82, Sydney, Australia.

Kolmogorov, A. N. [1942], Izv. Akad. Nauk SSR Ser Phys. VI, No. 1-2, p. 56.

Launder, B. E. and D. B. Spalding [1972], Lectures in Mathematical Models of Turbulence, Academic Press, New York.

Prandtl, L. [1945], Nachrichten von der Akad. der Wissenschaft in Göttingen, Germany.

☆U.S. GOVERNMENT PRINTING OFFICE: 1978-740-094/1239